Effect of Prior Athermal Martensite on the Isothermal Transformation Kinetics Below M_s in a Low-C High-Si Steel

A. NAVARRO-LÓPEZ, J. SIETSMA, and M.J. SANTOFIMIA

Thermomechanical processing of Advanced Multiphase High Strength Steels often includes isothermal treatments around the martensite start temperature (M_s). It has been reported that the presence of martensite formed prior to these isothermal treatments accelerates the kinetics of the subsequent transformation. This kinetic effect is commonly attributed to the creation of potential nucleation sites at martensite-austenite interfaces. The aim of this study is to determine qualitatively and quantitatively the effect of a small volume fraction of martensite on the nucleation kinetics of the subsequent transformation. For this purpose, dilatometry experiments were performed at different temperatures above and below the M_s temperature for athermal martensite in a low-carbon high-silicon steel. Microstructural analysis led to the identification of the isothermal decomposition product formed above and below M_s as bainitic ferrite. The analysis of the transformation processes demonstrated that the initial stage of formation of bainitic ferrite at heat treatments below M_s is at least two orders of magnitude faster than above M_s due to the presence of martensite.

I. INTRODUCTION

THE industrial sector is continuously looking for new steels for a range of applications. Those efforts have led to the development of a new generation of Advanced Multiphase High Strength Steels with very good combination of properties: high tensile strength and good ductility. Thermomechanical processing of these advanced multiphase steels often includes isothermal treatments around the martensite start temperature (M_s). When isothermal treatments are applied below the M_s temperature, a predetermined fraction of athermal martensite is present prior to the application of the isothermal treatment. This prior athermal martensite has an accelerating effect on the overall isothermal transformation close to the M_s temperature, which is generally known as the "swing-back" phenomenon.[1–4]

But, how can athermal martensite contribute to this acceleration? It is well known that martensite preferentially nucleates at prior-austenite grain boundaries, i.e., at austenite-austenite (γ-γ) interfaces.[5] In an isothermal treatment after quenching, the athermal martensite formation is stopped before the completion of the transformation and thus martensite-austenite (α'-γ) interfaces are present in the material, which can act as

potential nucleation sites.[6] Kawata et al.[5] reported that a further acceleration of the isothermal transformation above M_s is achieved by increasing the volume fraction of prior athermal martensite and, as a consequence, the density of α'-γ interfaces. However, the mechanisms of this acceleration are not well understood and the effect of these α'-γ boundaries on later transformation kinetics remains unclear.

Microstructures obtained in isothermal treatments around the M_s temperature depend on the chemical composition and the temperature of the isothermal holding. Above M_s, in hypoeutectoid steels, researchers agree about the nature of the isothermal product obtained from the decomposition of austenite. Microstructures are generally formed by a bainitic ferrite matrix with or without carbides, depending on the alloying elements and the isothermal holding time, and retained austenite, in the form of thin films or martensite-austenite (MA) islands.[7–13] The isothermally obtained phase product is generally called bainite. While the bainitic ferrite is free of carbides in upper bainite, lower bainitic ferrite can contain a fine dispersion of plate-like carbides, depending on the silicon content.[14]

However, below M_s, there is discussion about which phase product is obtained from the isothermal decomposition of austenite. Different observations have shown that isothermal products formed below the M_s temperature can be purely bainitic, purely martensitic or an isothermal product nor purely martensitic nor bainitic, as is explained below:

1. Kim et al.[13,15,16] state that the nature of the isothermal product obtained in 0.2C-1.5Mn-1.5Si (wt pct) alloys, after applying isothermal treatments

A. NAVARRO-LÓPEZ, Ph.D. Student, J. SIETSMA, Full Professor, and M.J. SANTOFIMIA, Associate Professor, are with the Department of Materials Science and Engineering, Delft University of Technology, Mekelweg 2, 2628 CD Delft, The Netherlands. Contact e-mail: a.navarrolopez@tudelft.nl

below M_s, is neither purely martensitic nor purely bainitic. The units of this characteristic product are, for instance, much wider than the laths in athermal martensite, and the boundaries are wavy and contain ledges. However, the presence of multivariant carbides in the isothermal product below M_s implies that it has clear similarities with athermal martensite.

2. Van Bohemen et al.[10] report that bainite can form below the martensite start temperature in a steel with 0.66 wt pct C. The microstructure obtained below the M_s temperature in a medium carbon alloy is formed by sheaves of lower bainite in a martensitic matrix and some blocks of tempered martensite exhibiting a typical multivariant carbide precipitation. This microstructure has been compared with one that was isothermally formed above the M_s temperature. A very similar bainitic microstructure is obtained in the form of long, thin sheaves containing carbides. Therefore, Van Bohemen et al. consider that the transformation product observed below M_s in their experiments is best described as bainite. Kinetics analysis supports this observation.

3. Kolmskog et al.[17] report that although it is possible that bainitic ferrite can form below the martensite start temperature, this bainitic ferrite grows slowly, similar to Widmanstätten ferrite growth above the M_s temperature. This explanation is linked to the controversy surrounding the bainite growth mechanisms. Two schools of thought differ about the mechanism of bainite formation. One argues that bainitic ferrite grows without diffusion of carbon by a displacive mechanism like martensitic growth; the transformation kinetics is thus determined by the nucleation process. The other school argues that bainitic ferrite nucleates and grows by a diffusion-controlled mechanism, like Widmanstätten ferrite; the transformation kinetics is thus governed by diffusion processes.

4. Oka and Okamoto[3] report the formation of isothermal martensite in treatments above and below the M_s temperature in hypereutectoid steels. Isothermal martensite was observed in the form of thin plates and/or leaf-like units. The formation of isothermal martensite has mainly been studied in high-nickel alloys and high-carbon steels,[18–20] but it has not been reported in hypoeutectoid steels.

As shown, there are several unresolved issues with respect the effect of prior athermal martensite on the subsequent isothermal transformations below M_s. Although this martensite introduces new potential nucleation sites in the form of martensite-austenite interfaces, their quantitative contribution to the subsequent transformation kinetics still remains unclear. In addition, the mechanisms involved in the accelerating effect of the prior athermal martensite in the later formation of an isothermal product are not fully clarified. Also, there is still controversy about the nature of the isothermal product obtained in isothermal treatments below the M_s temperature.

The goal of this study is to determine whether the presence of a small volume fraction of martensite affects the nucleation kinetics of the subsequent transformation, as well as to qualitatively and quantitatively determine this contribution to the subsequent transformation kinetics. This will provide insight into the microstructural mechanism that causes the acceleration of the transformation. Additionally, a microstructural study was performed in order to identify the transformation product formed during isothermal heat treatments above and below M_s. For this purpose, dilatometry experiments were performed at different temperatures above and below M_s in a low-carbon high-silicon steel.

II. EXPERIMENTAL PROCEDURE

The steel investigated was a hot rolled steel of composition 0.2C-3.51Mn-1.52Si-0.25Mo-0.04Al (wt pct). Manganese enhances the austenite stability and thus retards the formation of ferrite, pearlite, and bainite, which results in a shift of the TTT- and CCT-curves of these phases to longer times. The combination of low-carbon and high-silicon contents minimizes and delays the carbide precipitation during the isothermal holding. The as-received material was hot rolled into a 4mm-thick steel slab. Dilatometry specimens were taken from hot rolled slabs, parallel to the rolling direction. These were cylindrical of dimensions 10 mm in length and 3.5 mm in diameter. All specimens were heat-treated using a Bähr 805A dilatometer. The specimens were placed between two quartz rods, heated by an induction coil, and cooled using nitrogen gas. A thermocouple was spot-welded in the middle of the specimens to measure and control the temperature.

Two sets of heat treatments were applied:

(a) A direct-quench treatment was used to determine the experimental M_s temperature and the volume fraction of martensite as a function of temperature. The treatment consisted of heating to a fully austenitizing temperature 1173 K (900 °C) at a rate of 2 K s^{-1}, austenitization at 1173 K (900 °C) for 240 seconds, and cooling until room temperature at a cooling rate of 20 K s^{-1}. From this treatment, the experimental M_s was determined as $M_{s(1pct)}$ = 593 K (320 °C) ± 5 K, at which temperature the volume fraction of martensite formed is 1 pct.

(b) Isothermal treatments were performed at different temperatures above and below M_s to evaluate the effect of the previously formed athermal martensite on the subsequent isothermal transformation kinetics. The heat treatments consisted of heating at 2 K s^{-1} to a fully austenitizing temperature 1173 K (900 °C), austenitization at 1173 K (900 °C) for 240 seconds, cooling at 20 K s^{-1} until the isothermal temperature, ranging from 643 K to 543 K (370 °C to 270 °C) as shown in Figure 1, where the specimens were held for 3600 seconds. The heat treatments ended with a final cooling to room temperature at a rate of 20 K s^{-1}.

The heat-treated specimens were metallographically prepared by grinding and polishing. Nital 2 pct etching

was applied to the specimens to observe the phases formed by Light Optical Microscopy (LOM). Specimens were also analyzed with a JEOL JSM-6500F Scanning Electron Microscope (SEM) using a 15 kV electron beam and the Secondary Electron Imaging (SEI) detection mode. X-ray diffraction (XRD) experiments were performed on all specimens to determine the volume fraction of retained austenite (RA) at room temperature. These experiments were carried out in a Bruker D8-Advance diffractometer equipped with a Bruker Vantec Position Sensitive Detector. CoKα radiation was used in the 2θ scan from 40 to 130 deg with a step size of 0.035 deg. The fractions of austenite and ferrite were calculated by the integrated area method using the (111), (200), (220), and (311) austenite peaks, and the (110), (200), (211), and (220) ferrite peaks.[21]

III. RESULTS AND DISCUSSION

A. Martensite Fraction and M_s Temperature

Having as much information as possible on the evolution of the martensite volume fraction and the M_s temperature is crucial to qualitatively and quantitatively determine the effect of prior athermal martensite
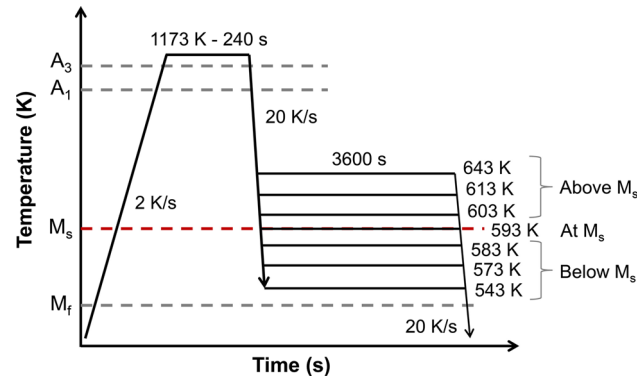

Fig. 1—Schematic representation of heat treatments applied to the selected steel.
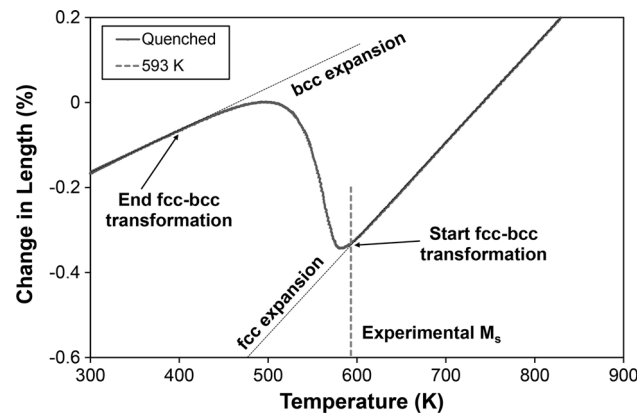

Fig. 2—Change in length vs temperature during cooling at 20 K s^{-1}.

on the subsequent formation of bainitic ferrite. Figure 2 shows the change in length as a function of temperature during cooling obtained from the quench treatment. The martensite volume fractions formed during cooling to different temperatures below M_s were calculated applying the lever rule to that curve. The contraction occurring during cooling from austenitization to the M_s temperature follows a straight line, which indicates that ferrite, pearlite, and bainite are not forming before the martensitic transformation. The dilatation below the M_s temperature is characteristic for fcc-bcc transformation indicating the formation of athermal martensite. The M_s temperature was calculated from the dilatometric curve represented in Figure 2. The experimental M_s temperature for the alloy studied was determined at 593 K (320 °C) ± 5 K, at which the volume fraction of martensite formed was 1 pct.

Figure 3 shows the evolution of the experimental volume fraction of martensite obtained after applying the lever rule to the curve of Figure 2. A comparison with the theoretical fitting of the Koistinen and Marburger model (KM) is also displayed. The KM model[22] quantitatively describes the progress of the austenite-martensite transformation as

$$f^{\alpha'} = 1 - \exp\left[-\alpha_m \cdot \left(T_{KM} - T_q\right)\right], \qquad [1]$$

where $f^{\alpha'}$ is the volume fraction of martensite formed at a temperature T_q below the M_s temperature, T_{KM} is the theoretical martensite start temperature, which is typically somewhat lower than the experimentally determined M_s, and α_m is the rate parameter.[23] T_{KM} and α_m are taken as fitting parameters. In this case, the values of T_{KM} and α_m obtained from the fit are 577 K (304 °C) and 0.035 K^{-1}, respectively. This model was not finally considered for determining the M_s temperature as it does not provide accurate values at the very beginning of the martensite transformation (see Figure 3).[23]

B. Microstructure

Figure 4 shows the microstructures of the specimens after isothermal treatments for 3600 seconds at 643 K,
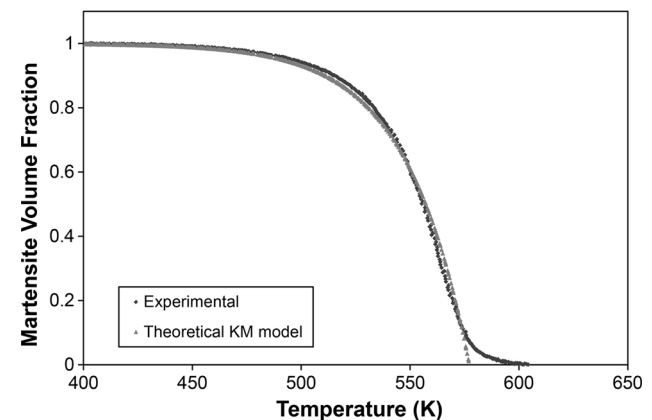

Fig. 3—Experimental volume fraction of martensite calculated applying the lever rule and fitting of this volume fraction by the Koistinen and Marburger model.
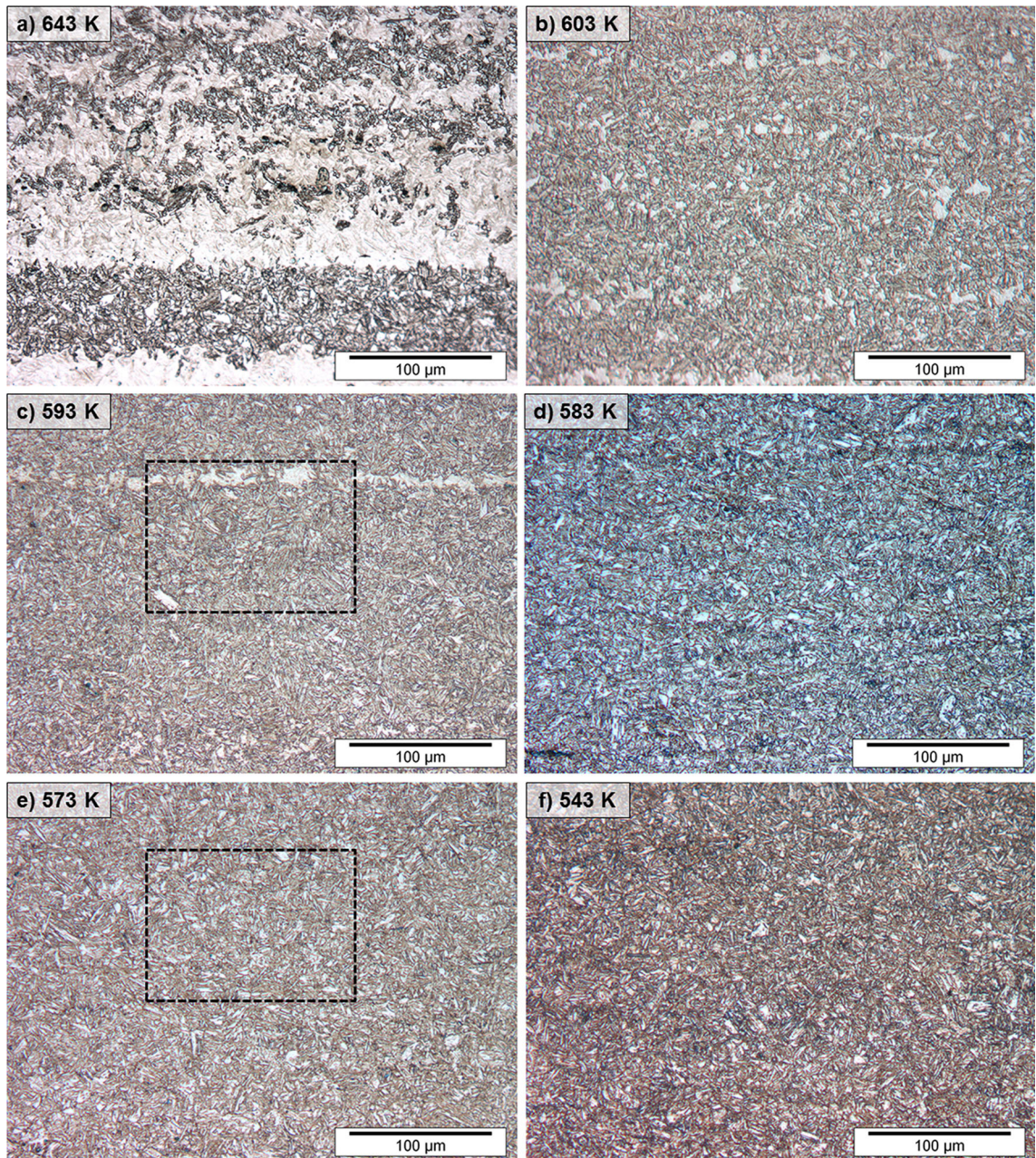
Fig. 4—Microstructures after isothermal treatments for one hour at temperatures above M_s, (a) 643 K (370 °C) and (b) 603 K (330 °C), just at M_s, (c) 593 K (320 °C), and below M_s, (d) 583 K (310 °C), (e) 573 K (300 °C), and (f) 603 K (330 °C). The dashed rectangles are enlarged in Figs. 5(a) and (b), respectively.

603 K, and 593 K (370 °C, 330 °C, and 320 °C) (above and just at M_s) and at 583 K, 573 K, and 543 K (310 °C, 300 °C, and 270 °C) (below M_s).

A structure formed by alternating bands of bainitic ferrite and martensite can be clearly observed in microstructures obtained at 643 K, 603 K, and 593 K (370 °C, 330 °C, and 320 °C) (above or just at M_s). Microstructural banding is a very common characteristic in hot-rolled low-carbon high-alloyed steels. This phenomenon occurs due to the segregation of substitutional alloying elements during dendritic solidification.

After processes such as hot rolling, areas with different segregation levels will align in the form of bands following the rolling direction. In this case, the high manganese content and its heterogeneous distribution explain the microstructures obtained. Manganese is a γ-stabilizer and decreases the A_3 and M_s temperatures. The M_s temperature is locally affected by banding, so it will be lower in Mn-rich areas than in Mn-poor ones. This implies that athermal martensite will firstly form in Mn-poor areas. Therefore, since the M_s temperature is defined as $M_{s(1pct)}$, this means that a 1 pct volume
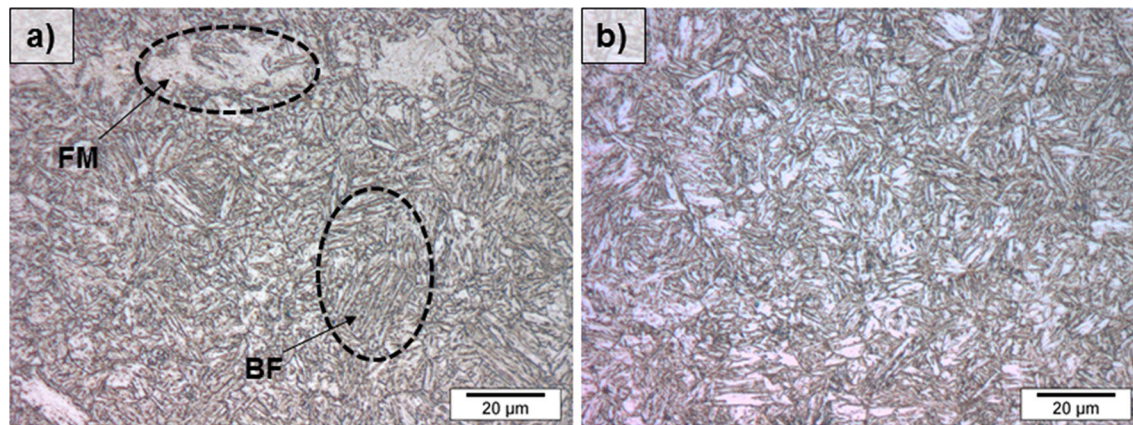
Fig. 5—Enlarged images of the area surrounded by dashed squares in Figs. 4(c) and (e), corresponding to the microstructures obtained in specimens isothermally treated for 3600 s: (a) just at M_s at 593 K (320 °C), and (b) below M_s at 573 K (300 °C). Bainitic Ferrite is indicated by BF, and Fresh Martensite by FM.

fraction of athermal martensite has already formed and, due to banding, the formation of that martensite has probably taken place at Mn-poor areas.

Due to the Mn γ-behavior, austenite is thus more stable in Mn-rich areas, and bainitic ferrite will first grow in the areas where the Mn content is lower. After the isothermal treatment, some of the remaining untransformed austenite will transform into fresh martensite in the final cooling to room temperature. Although microstructural bands are not visible below M_s [583 K, 573 K, and 543 K (370 °C, 330 °C, and 320 °C)], Mn segregation is also present in these specimens.

Figure 4 shows that as the isothermal temperature decreases, from 643 K to 543 K (370 °C to 270 °C), the microstructures appear more homogeneous and microstructural bands are thinner, whereas they cannot be distinguished below M_s. A possible explanation of this is related with the undercooling at the transformation temperatures with respect to the A_3 temperature. When the undercooling is higher (lower transformation temperature), the driving force for the transformation is also higher, and the difference in terms of this driving force between Mn-rich and Mn-poor areas is not so pronounced as at high temperature. Thus, the effect of the inhomogeneous distribution of Mn on the microstructure development is smaller.

In isothermal treatments above and just at M_s, bainitic ferrite (BF) appears in the form of sheaves of acicular units of ferrite and can be distinguished from the fresh martensite (FM) formed in the final cooling, as shown in Figure 5(a). Fresh martensite is observed in the form of irregular areas within the banded structure. However, below M_s, it is rather difficult to differentiate between tempered martensite, bainitic ferrite, and fresh martensite (see Figure 5(b)). Tempered martensite in the microstructures refers to prior athermal martensite formed during cooling to the isothermal holding temperature. This martensite is tempered to some extent during the isothermal treatments. Acicular units of bainitic ferrite are not clearly identified and can be

confused with laths of tempered martensite. Retained austenite can also be present in these microstructures in the form of interlath films between bainitic ferrite units, and/or as coarser particles. This retained austenite as well as carbides cannot be clearly distinguished by optical microscopy due to its nanometric size.

To clarify the nature of the isothermal product obtained in treatments around M_s, three specimens treated at 613 K (340 °C) (above M_s), at 593 K (320 °C) (just at M_s) and at 573 K (°C) (below M_s) were analyzed by scanning electron microscopy (SEM). Figure 6 shows that, at 613 K (340 °C; above M_s), the microstructure is a mixture of bainitic ferrite, retained austenite, and MA islands. Bainitic ferrite mainly appears in the form of acicular units with interlath retained austenite. MA islands with irregular shape can also be distinguished. Carbides are not identified in this microstructure.

At 593 K (320 °C; just at M_s), acicular units of bainitic ferrite with interlath retained austenite appear in the microstructure, as shown in Figure 7(a). Irregular-shaped MA islands can also be distinguished in both figures. These microstructures are similar to those obtained at temperatures above M_s. In Figure 7(b), a lath-shaped phase product with carbides within the lath can be observed. This product could be identified as either lower bainite or tempered martensite, so it is labeled as LB/TM in the micrographs. In this case, carbides are aligned in the same direction within the lath, which is argued to be characteristic of lower bainite microstructures. However, at this temperature, a very small fraction of prior athermal martensite might have formed during cooling from austenitization. If this were so, this martensite would temper during the isothermal holding and could be confused with bainitic ferrite.

Figures 8(a) and (b) show that, at 573 K (300 °C; below M_s), acicular units appear in similar structures as the bainitic ones identified in Figures 6 and 7. This indicates the formation of bainitic ferrite in isothermal treatments below M_s with similar morphological characteristics to that formed in treatments above and just at M_s. LB/TM can also be distinguished in Figure 8(c).

This product contains carbides aligned in the same direction within the lath, similar to the product observed just at M_s, at 593 K (see Figure 7(b)).

At 573 K (300 °C), a volume fraction of 16 pct athermal martensite has previously been formed during the cooling to this temperature. This martensite is tempered during the isothermal holding. Tempered Martensite (TM) is clearly observed in Figure 8(d). This phase product appears in the form of lath units with multivariant carbides within them. Below M_s, Figures 8(a) and (c) show other different structures, in the shape of blocks, with almost no carbides within them. These structures might be formed by different subunits of a phase product or be a unique coarse one.

C. Isothermal Transformation Kinetics

Figures 9(a) and (b) show the change in length of the specimens as a function of temperature during cooling for the specimens isothermally treated: (a) at 643 K, 613 K, 603 K (370 °C, 340 °C, 330 °C) (above M_s), and 593 K (320 °C) (just at M_s), and (b) at 583 K, 573 K, and 543 K (310 °C, 300 °C, and 270 °C) (below M_s). Above M_s, there is a linear contraction during cooling until the isothermal temperature is reached. An increase of the thermal length takes place during the isothermal holding, as shown in Figure 9(a). This indicates the formation of the isothermal product previously identified by SEM as bainitic ferrite.

However, below M_s, a deviation occurs from the linear contraction during cooling before the isothermal temperature is reached (see Figure 9(b)). This means that a fraction of prior athermal martensite has formed. In these cases, once the isothermal temperature is reached, the prior athermal martensite stops forming, and an increase of the change in length takes place due to the formation of the isothermal product. All experimental curves exhibit a non-linear change in length during quenching after the isothermal holding. This indicates the formation of martensite during the final cooling to room temperature. The isothermal transformation is thus an incomplete reaction. The remaining austenite is not sufficiently stable and will partially transform into fresh martensite, as can be observed in SEM micrographs (Figures 6, 7, and 8).

In order to quantify the fresh martensite fractions,[24,25] the net dilatations at 298 K (25 °C) of all isothermal treatments are compared with the maximum
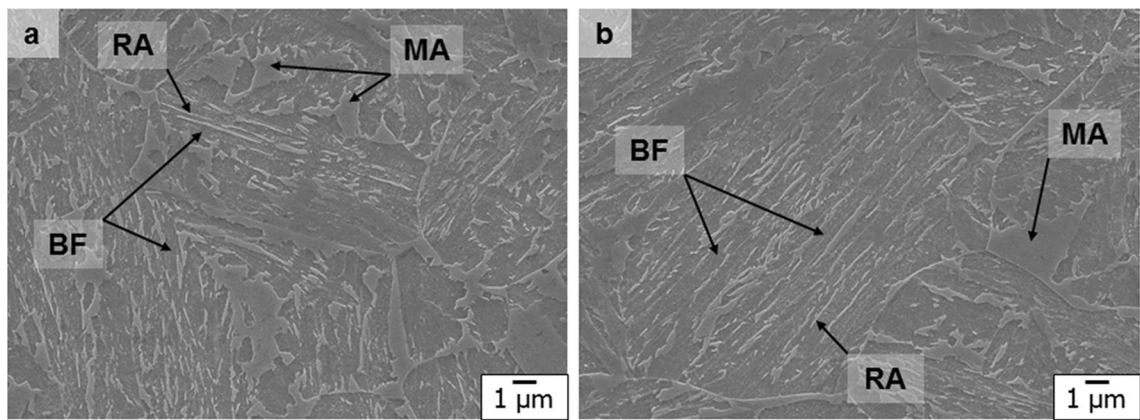

Fig. 6—Microstructures obtained in a specimen isothermally treated above M_s at 613 K (340 °C) for 3600 s. Bainitic Ferrite is indicated by BF, Martensite-Austenite islands by MA, and Retained Austenite by RA.
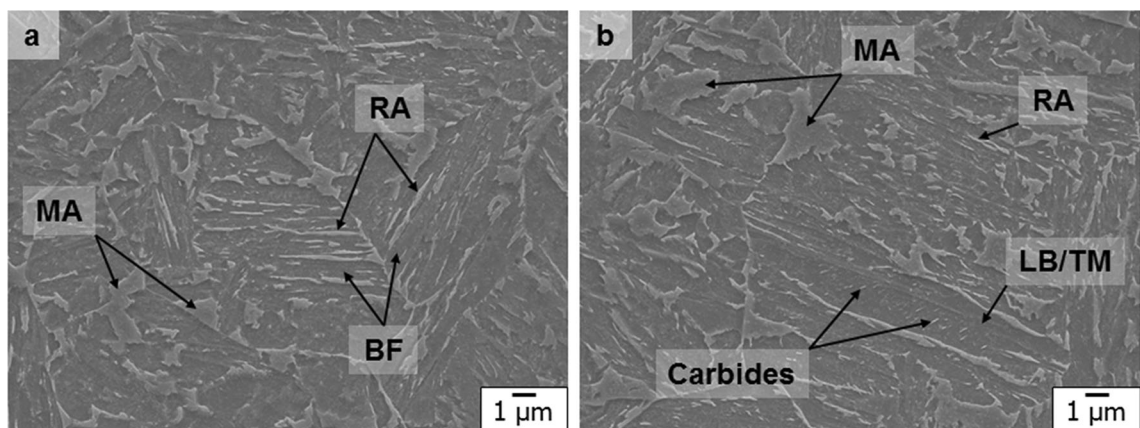

Fig. 7—Different microstructures obtained in a specimen isothermally treated just at M_s at 593 K (320 °C) for 3600 s. Bainitic Ferrite is indicated by BF, Martensite-Austenite islands by MA, Retained Austenite by RA, and Lower Bainite or Tempered Martensite by LB/TM.
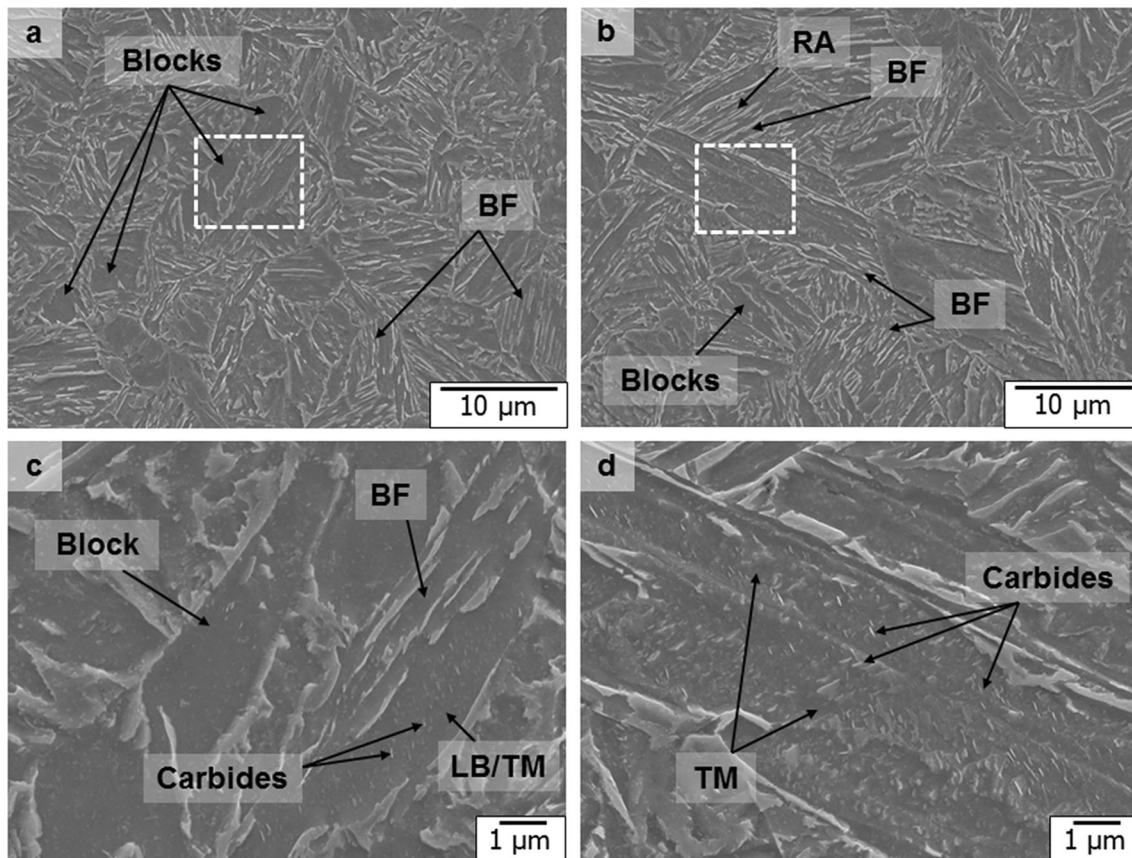
Fig. 8—(a) and (b) Microstructures obtained in a specimen isothermally treated below M_s at 573 K (300 °C) for 3600 s. (c) and (d) Enlarged images of the area surrounded by a dashed square in (a) and (c), respectively. Bainitic Ferrite is indicated by BF, Retained Austenite by RA, Lower Bainite or Tempered Martensite by LB/TM, and Tempered Martensite by TM.
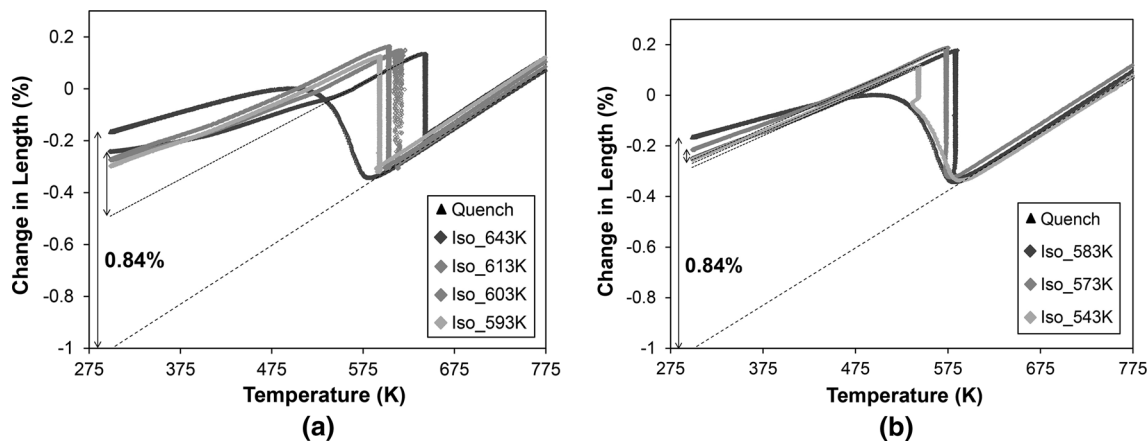

Fig. 9—Change in length as a function of temperature for isothermal treatments above and just at M_s (a) at 643 K, 613 K, 603 K, and 593 K, (370 °C, 340 °C, 330 °C, and 320 °C) and below M_s (b) at 583 K, 573 K, and 543 K (310 °C, 300 °C, and 270 °C).

net dilatation with respect to the austenitic phase obtained at the same temperature in the direct-quench treatment, which is 0.84 pct (see Figure 9). Net dilatations (indicated by double-ended arrows) are obtained calculating the difference of change in length between the experimental curves and the dashed lines. These dashed lines indicate the linear length change in case of absence of the martensitic transformation during

cooling. XRD results show that the volume fraction of retained austenite in the directly quenched specimen is approximately 1 pct, so the formation of 99 pct martensite leads to a net dilatation of 0.84 pct. The fractions of fresh martensite and retained austenite determined for all specimens are given in Figure 10. Bainitic ferrite volume fractions are calculated balancing the fractions of prior athermal martensite, retained
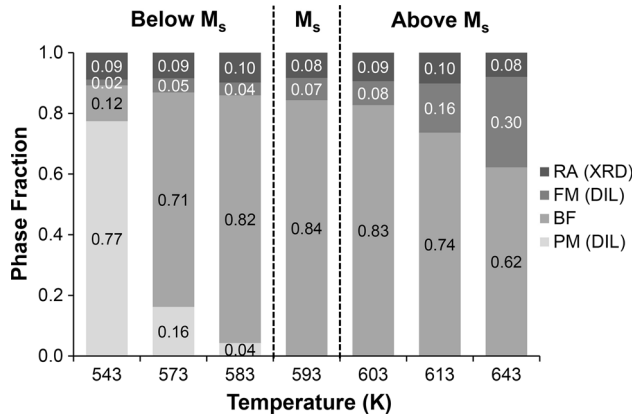
Fig. 10—Phase fractions obtained after the application of selected heat treatments including isothermal treatments at temperatures above, just, and below M_s. Prior athermal Martensite is indicated by PM, Bainitic Ferrite by BF, Fresh Martensite by FM, and Retained Austenite by RA.

austenite, and fresh martensite formed in the final cooling to room temperature.

Before analyzing the experimental kinetic curves of the isothermal formation of bainitic ferrite, a "zero" (start) time and change in length must be established. First, a cubic spline interpolation is applied to the length data measured by dilatometry in order to obtain a value for a fixed incremental time interval. After that, the resulting data are smoothed by moving average to decrease the scatter. Finally, above M_s, the start of the isothermal transformation is considered at the minimum change in length since it is assumed that there is no transformation until the change in length becomes positive. Below M_s, the start of the isothermal transformation corresponds to the point of minimum temperature reached during cooling when athermal martensite stops forming.

Figure 11 shows the bainite fraction obtained during the isothermal treatments at each temperature by means of dilatometry. The transformation kinetics above M_s increases as the temperature decreases and approaches M_s [593 K (320 °C) ± 5 K]. Above and just at M_s (Figure 11(a)), bainitic transformation kinetics follows an S-shape curve which is shifted to shorter times as the temperature of the treatment decreases. The maximum fraction of bainitic ferrite increases with the decrease of the holding temperature. Below M_s (Figure 11(b)), the shape of the curves changes and the isothermal transformation instantaneously reaches the maximum transformation rate. The highest bainitic ferrite fractions are reached in a range of ±20 K around M_s. The temperature dependence of the maximum fractions of bainitic ferrite is observed in Figure 10.

The change in the kinetics of the bainitic ferrite formation above and below M_s is highlighted in Figure 12. This figure shows the bainitic ferrite formation as a function of time during two isothermal holdings at 603 K (330 °C), just above M_s, and at 583 K (310 °C), just below M_s. In these treatments, the fraction of bainitic ferrite formed is very similar, around 82 pct (see Figure 10). However, the shape of the curves

is different, changing from an "S" curve at 603 K (330 °C) without any athermal martensite formation, to an initially rapidly ascending curve at 583 K (310 °C), when there is a small fraction of prior athermal martensite formed (approximately 4 pct). This confirms that at an early stage, the transformation at 583 K (310 °C) (below M_s) is much faster than that at 603 K (330 °C) (above M_s) and that the presence of martensite strongly accelerates the subsequent isothermal transformation kinetics.

The effect of prior athermal martensite on the bainitic ferrite formation is studied in terms of nucleation rate and density of potential nucleation sites, assuming that the bainitic ferrite growth mechanism is governed by nucleation without diffusion of carbon. The variation of bainitic ferrite fraction (f^B) with time (t) can be described by Reference 6:

$$\frac{df^B}{dt} = \frac{dN}{dt} \cdot V_u, \qquad [2]$$

where dN/dt is the nucleation rate per unit of volume and V_u is the average volume of a bainitic subunit. This volume is sometimes assumed constant with temperature in the literature, with dimensions of $0.2 \times 10 \times 10\ \mu m^3$,[26] but investigations have shown that the average volume of a bainitic subunit actually depends on different factors, such as temperature, austenite strength, and driving force, as described by Singh and Bhadeshia.[27] Parker[28] empirically modeled the bainitic subunit thickness as a temperature-dependent parameter, based on previous experimental work of Chang and Bhadeshia[29] on silicon-rich steels with carbon contents between 0.095 and 0.5 wt pct, isothermally treated between 523 K and 773 K (250 °C and 500 °C). The thickness of bainitic subunits, z', was then modeled as

$$z' = z_0 \cdot \frac{(T - 528\,\text{K})}{150\,\text{K}}, \qquad [3]$$

where T is the isothermal holding temperature in Kelvin and z_0 is a reference thickness. Assuming that bainitic ferrite has a plate shape and all the plate dimensions vary with temperature as described in Eq. [3], the volume of bainitic subunits can be described as[26]

$$V_u = V_0 \cdot \left(\frac{T - 528\,\text{K}}{150\,\text{K}}\right)^3, \qquad [4]$$

where V_0 is the previously mentioned volume of $0.2 \times 10 \times 10\ \mu m^3$. In this study, the nucleation rate (dN/dt) is calculated from Eq. [2] for all isothermal treatments using the experimental data for df^B/dt and considering that the volume of the bainitic subunits changes with the applied temperature as described in Eq. [4]. This latter equation can be used for the steel studied and the isothermal treatments performed since the composition is within the above-mentioned ranges and temperatures are higher than 528 K.

The evolution of the nucleation rate in different treatments above and below M_s, obtained from the
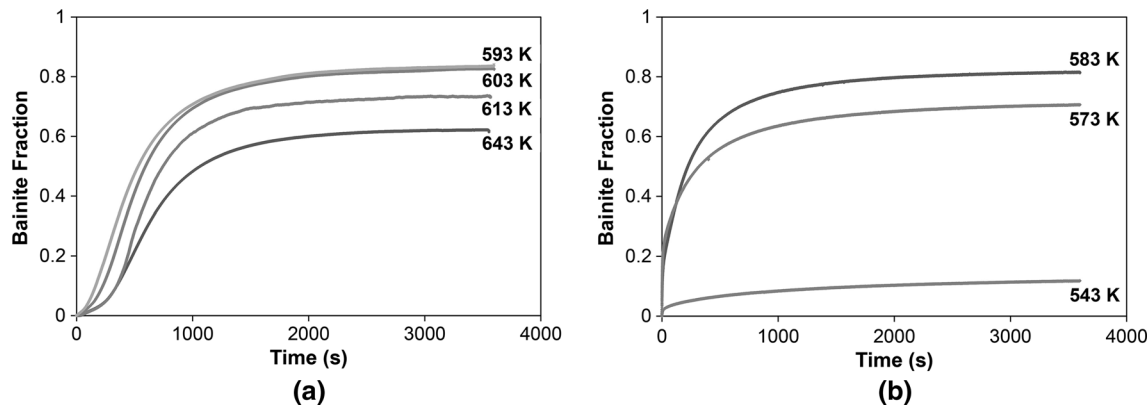
Fig. 11—Volume fractions of bainitic ferrite as a function of isothermal holding time at different temperatures above and just at M_s (a) and below M_s (b).
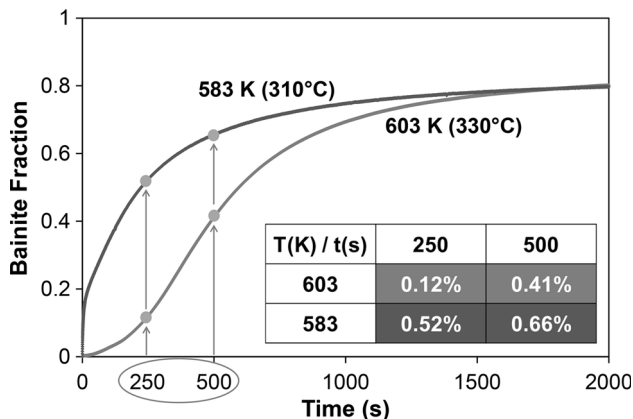

Fig. 12—Bainite fractions as a function of time at 603 K and 583 K (330 °C and 310 °C), above and below the M_s temperature, respectively.

fraction curves of Figure 11 and Equations [2] and [4], is observed in Figure 13. In treatments above and just at M_s, for instance at 603 K and 593 K (330 °C and 320 °C) (Figure 13(a)), the nucleation rate increases rapidly until reaching a maximum at bainitic ferrite fractions between 0.20 and 0.30 vol. This maximum coincides with the inflection point of the experimental S-shaped kinetic curve of the bainitic ferrite formation (see Figure 12). Then, the decrease of nucleation rate is gradual until the formation of the maximum bainitic ferrite fraction is completed. In treatments below M_s, at 583 K and 573 K (310 °C and 300 °C) (Figure 13(b)), the maximum nucleation rate is obtained at the very beginning of the transformation and it is 2 to 3 orders of magnitude higher than that of treatments above M_s. The nucleation rate decreases rapidly until reaching similar values to those obtained in treatments above M_s.

Figure 13(a) also shows that the nucleation rate increases as the isothermal temperature decreases. This fact is in good agreement with the shift of bainite fraction curves to shorter times as shown in Figure 11(a). The lower the isothermal temperature, the higher the undercooling, so the driving force for nucleation will be higher, increasing the transformation kinetics. Consequently, a faster transformation implies a

smaller size of the bainitic subunits, which is in accordance with Eq. [4] used for the nucleation rate calculations. If this reflection is applied to the isothermal treatments below M_s, in conjunction with the increment of the density of potential nucleation sites introduced by the prior athermal martensite, the nucleation rate in those treatments will be much faster, as observed in Figure 13(b). The higher density of nucleation sites facilitates a faster isothermal bainite kinetics, even when the formed units are smaller.

Table I shows the theoretical values of the volume of the bainitic subunits (V_u) as well as the experimental values of nucleation rate $(dN/dt)_{0.5}$, calculated by Eq. [2], at 0.5 seconds after the start of the isothermal transformation for all heat treatments. The elapsed time selected has been 0.5 seconds in order to only study the effect of prior martensite on the nucleation rate, minimizing the autocatalytic nucleation effects. Autocatalytic nucleation is related to the induced formation of new nuclei due to the stresses and strains introduced after the formation of a phase product, in this case, prior athermal martensite.

A logarithmic representation of the initial nucleation rates $(dN/dt)_{0.5}$ for all isothermal transformations is shown in Figure 14. The M_s temperature represents an inflection point in the initial nucleation rate since it changes sharply from temperatures just above M_s to those just below M_s. The nucleation rates below M_s are on the order of 10^{16} m^{-3} s^{-1} or higher. Above M_s, the nucleation rates are on the order of 10^{14} m^{-3} s^{-1} or less. Therefore, small fractions of athermal martensite prior to isothermal treatments below M_s increase the nucleation rate by at least two orders of magnitude at the start of the subsequent isothermal transformations, compared to those above M_s where prior martensite does not form. This confirms the differences described in the evolution of the bainitic ferrite formation and the nucleation rates above and below M_s, as shown in Figures 12 and 13, respectively.

As the prior athermal martensite volume fraction increases, the nucleation rate of bainitic ferrite at α'-γ interfaces at the start of the transformation also increases. This means that the volume fraction of bainitic ferrite formed after 0.5 seconds will be higher
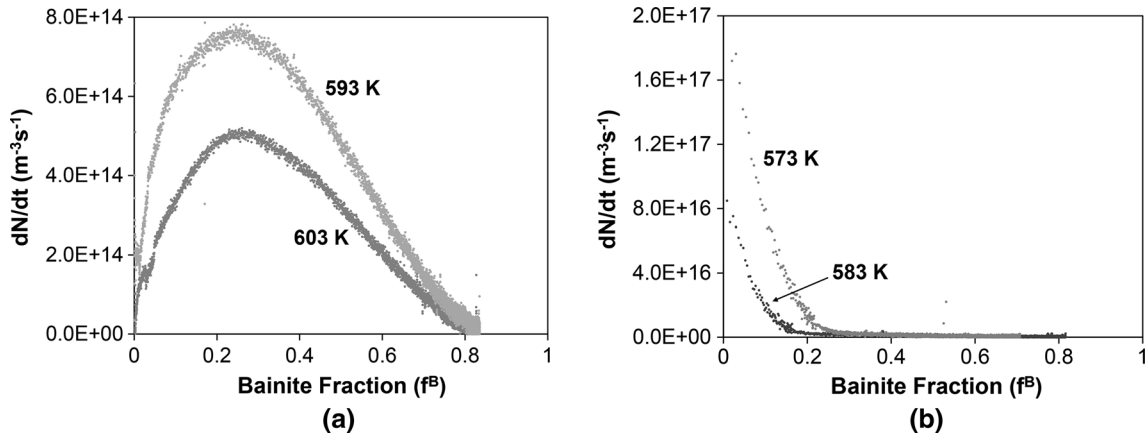
Fig. 13—Evolution of nucleation rates during different isothermal holdings at temperatures above and just at M_s (a) and below (b) the M_s temperature, assuming a temperature-dependent volume of the bainitic subunits.

Table I. Calculated and Experimental Values of Different Parameters Obtained for the Isothermal Treatments Performed at Temperatures Above, Just, and Below M_s. V_u (Volume of Bainitic Subunits), f^{PM} (Fraction of Prior Athermal Martensite), t_i (Elapsed Time Since the Start of the Isothermal Transformation), $(dN/dt)_{0.5}$ (Nucleation Rate at $t_i = 0.5$ s), n_{sites} (Number of Nuclei Forming Per Second and Austenite Grain at t_i), and f^{BF} (Experimental Volume Fraction of Bainitic Ferrite Formed After t_i)

Temperature [K (°C)]	V_u (m³)	f^{PM}	t_i (s)	$(dN/dt)_{0.5}$ (m⁻³ s⁻¹)	n_{sites} (s⁻¹)	f^{BF}
643 (370)	9.0×10^{-18}	0	0.5	1.9×10^{12}	1.0×10^{-3}	8.8×10^{-6}
613 (340)	3.7×10^{-18}	0	0.5	3.2×10^{12}	1.7×10^{-3}	5.9×10^{-6}
603 (330)	2.5×10^{-18}	0	0.5	2.5×10^{14}	1.3×10^{-1}	1.1×10^{-3}
593 (320)	1.6×10^{-18}	0	0.5	1.3×10^{14}	6.7×10^{-2}	1.3×10^{-4}
583 (310)	9.9×10^{-19}	0.04	0.5	6.2×10^{16}	32	3.6×10^{-2}
573 (300)	5.5×10^{-19}	0.16	0.5	1.4×10^{17}	74	4.6×10^{-2}
543 (270)	2.1×10^{-20}	0.77	0.5	4.9×10^{17}	255	6.8×10^{-3}

due to a faster transformation kinetics. However, to understand why the transformation kinetics increases, it is necessary to determine the relationship between the volume fraction of prior athermal martensite, the interfaces involved in the transformation, and the bainitic ferrite fraction formed. To tackle this problem, a new variable has been defined, which is called as n_{sites}. This variable represents the number of nucleation events per second and austenite grain. Experimental values of n_{sites} at $t_i = 0.5$ seconds since the start of the isothermal transformations are listed in Table I. These values have been calculated by multiplying the nucleation rate (dN/dt) by the average volume of an austenite grain (V^γ_{grain}), as expressed by

$$n_{sites}(t_i) = \left(\frac{dN}{dt}\right)_{t_i} \cdot V^\gamma_{grain} \qquad [5]$$

The austenite grain diameter has been determined by SEM, obtaining an average value of 10 μm. Above M_s, γ-γ interfaces are the only potential nucleation sites at the start of the isothermal transformations. Below M_s, γ-γ interfaces and also α'-γ interfaces will provide potential nucleation sites for the bainitic ferrite formation. Assuming that there is no contribution of nucleation sites from bainite-austenite (α^b-γ) interfaces at the very beginning of isothermal transformations, the
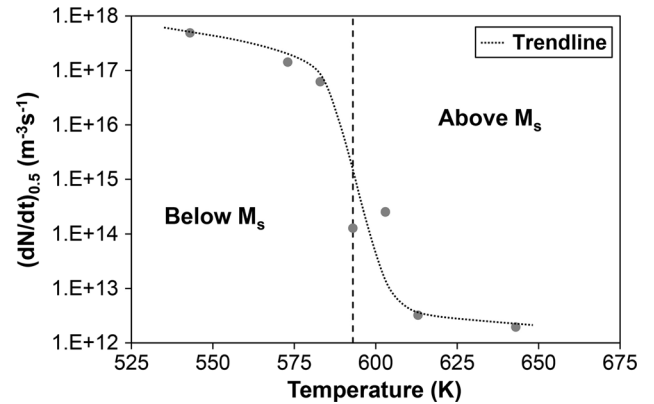

Fig. 14—The initial nucleation rate as a function of the isothermal temperature at 0.5 s after the start of the isothermal transformations above, just, and below M_s.

difference in the values of n_{sites} between treatments above and below M_s can be attributed to α'-γ interfaces, due to the presence of prior athermal martensite, and to a temperature difference itself, from which the driving force will increase as temperature decreases. If comparing treatments above M_s with those below M_s, differences in n_{sites} are more than two orders of magnitude higher than those obtained comparing treatments only above or only below M_s. Although the temperature
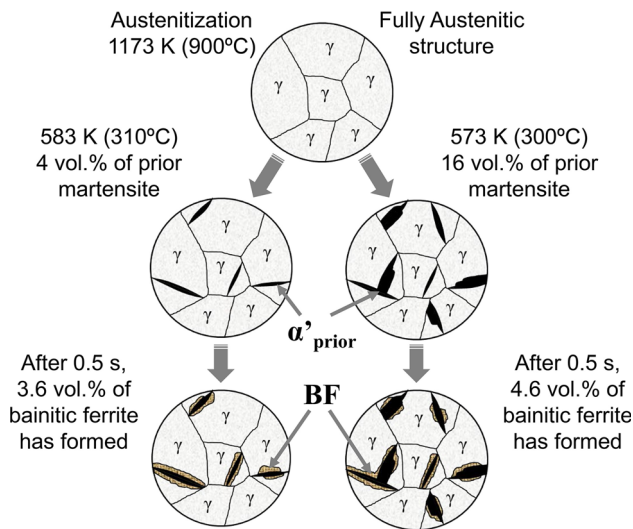
Fig. 15—Schematic evolution of the initial microstructure at the very beginning of the isothermal holding at temperatures 583 K and 573 K (310 °C and 300 °C), both below M_s.

difference will contribute to the transformation kinetics, the increase of the density of nucleation sites has a stronger contribution to the nucleation rate at the beginning of the isothermal transformation below M_s.

Table I shows that, in treatments below M_s, n_{sites} does not increase proportionally to the martensite volume fraction. To clarify the relationship between martensite fraction and nucleation behavior, a diagram of the evolution of the initial microstructure from the austenitization until 0.5 seconds after the start of the isothermal transformation at 583 K and 573 K (310 °C and 300 °C) is shown in Figure 15. The values presented are extracted from Table I. At 1173 K (900 °C), the microstructure is fully austenitic. In the subsequent cooling until temperatures below M_s, 583 K and 573 K (310 °C and 300 °C), small fractions of athermal martensite form depending on the quenching temperature. After 0.5 seconds, a small fraction of bainitic ferrite has formed, and that fraction is different depending on the prior athermal martensite fraction.

As observed in Table I, the increase of the volume fraction of bainitic ferrite formed after 0.5 seconds at lower temperatures is not proportional to the volume of prior athermal martensite previously formed. The reason is that the subunits of bainitic ferrite nucleate at α'-γ interfaces, so the nucleation process will depend on the interfacial area, rather than on the volume fraction of athermal martensite. Hence, the arrangement of martensite units within the austenite grain should be considered. Martensite generally forms in clusters or blocks, and not in the form of individual units homogeneously distributed in the material (see Figures 8(b) and (d)). For this reason, n_{sites} does not increase in the same proportion as the volume fraction of prior athermal martensite. Experimental results (Table I) suggest a relationship between n_{sites} and $(f^{PM})^{2/3}$ at the very beginning of the isothermal transformations below M_s. This indicates that the α'-γ interfacial area plays a

dominant role in the transformation kinetics in treatments below M_s. Further investigations are required for a better understanding of the mentioned relationship.

The acceleration effect of prior athermal martensite on the bainitic ferrite formation could lead to significant advantages in steel technology. Bainitic steels could be created through much faster processing routes; these steels can be manufactured with the same fractions of bainitic ferrite by heat treatments below M_s in less time than above M_s. The good combination of mechanical properties would be very similar to bainitic steels obtained above M_s; small fractions of prior athermal martensite can provoke a strong accelerating effect on the subsequent transformation, and prior martensite would be tempered without adding brittleness.

IV. CONCLUSIONS

The effect of prior athermal martensite and its contribution to the subsequent transformation kinetics was qualitatively and quantitatively determined in isothermal treatments below M_s in a low-C high-Si steel. The main conclusions obtained are the following:

1. Bainitic ferrite was identified as the isothermal product formed in treatments below M_s, where prior athermal martensite had already formed. This bainitic ferrite appears in the form of acicular units with interlath retained austenite, similar morphological characteristics to that obtained in treatments above and just at M_s.
2. A phase product with morphological similarities to lower bainite and/or tempered martensite was identified in treatments below and just at M_s. This product appears in the form of laths containing carbides aligned in the same direction
3. Prior athermal martensite has a strong accelerating effect on the subsequent isothermal transformation kinetics due to the creation of a high number of nucleation sites in the form of martensite-austenite (α'-γ) interfaces.
4. Small fractions of prior athermal martensite cause an acceleration by at least two orders of magnitude of the nucleation rate at the start of the subsequent isothermal transformations below M_s, compared to those above M_s where prior martensite does not form.
5. There appears to be a relationship between the initial nucleation rate at each temperature and the martensite-austenite interfacial area, confirming the important role of martensite-austenite interfaces on the subsequent isothermal transformation kinetics.

OPEN ACCESS

REFERENCES

1. R.T. Howard and M. Cohen: *Trans. AIME*, 1948, vol. 176, pp. 384–97.
2. S.V. Radcliffe and E.C. Rollason: *J. Iron Steel Inst.*, 1959, vol. 191, pp. 56–65.
3. M. Oka and H. Okamoto: *Metall. Trans. A*, 1988, vol. 19A, pp. 447–52.
4. D.H. Kim, J.G. Speer, H.S. Kim, and B.C. De Cooman: *Metall. Mater. Trans. A*, 2009, vol. 40A, pp. 2048–60.
5. H. Kawata, K. Hayashi, N. Sugiura, N. Yoshinaga, and M. Takahashi: *Mater. Sci. Forum*, 2010, vols. 638–642, pp. 3307–12.
6. M.J. Santofimia, S.M.C. Van Bohemen, D.N. Hanlon, L. Zhao, and J. Sietsma: *Inter. Symp. on AHSS, 2013*, AIST. 2013, pp. 331–39.
7. K. Sugimoto, T. Ilda, J. Sakaguchi, and T. Kashima: *ISIJ Int.*, 2000, vol. 40, pp. 902–08.
8. K. Sugimoto, M. Murata, and S.M. Song: *ISIJ Int.*, 2010, vol. 50, pp. 162–68.
9. Y Jiang, R Zhou, R Zhou, D Lu, and Z Li: *Mater. Sci. Forum*, 2005, vols. 475–479, pp. 93–96.
10. S.M.C. Van Bohemen, M.J. Santofimia, and J. Sietsma: *Scripta Mater.*, 2008, vol. 58, pp. 488–91.
11. J.C. Hell, M. Dehmas, S. Allain, J.M. Prado, A. Hazotte, and J.P. Chateau: *ISIJ Int.*, 2011, vol. 51, pp. 1724–32.
12. I.A. Yakubtsov and G.R. Purdy: *Metall. Mater. Trans. A*, 2012, vol. 43A, pp. 437–46.
13. D Kim, JG Speer, and BC De Cooman: *Mater. Sci. Forum*, 2010, vols. 654–656, pp. 98–101.
14. M. Takahashi and H.K.D.H. Bhadeshia: *Mater. Sci. Technol.*, 1990, vol. 6, pp. 592–603.
15. D. Kim, J.G. Speer, and B.C. De Cooman: *Metall. Mater. Trans. A*, 2011, vol. 42A, pp. 1575–85.
16. D. Kim, S.J. Lee, and B.C. De Cooman: *Metall. Mater. Trans. A*, 2012, vol. 43A, pp. 4967–83.
17. P. Kolmskog, A. Borgenstam, M. Hillert, P. Hedstrom, S.S. Babu, H. Terasaki, and Y.I. Komizo: *Metall. Mater. Trans. A*, 2012, vol. 43A, pp. 4984–88.
18. S.R. Pati and M. Cohen: *Acta Metall.*, 1969, vol. 17, pp. 189–99.
19. A. Borgenstam, M. Hillert, and J. Agren: *Acta Metall. Mater.*, 1995, vol. 43, pp. 945–54.
20. A. Borgenstam and M. Hillert: *Acta Mater.*, 1997, vol. 45, pp. 651–62.
21. C.F. Jatczak, J.A. Larson, and S.W. Shin: SAE Special Publication 453, 1980.
22. D.P. Koistinen and R.E. Marburger: *Acta Metall.*, 1959, vol. 7, pp. 59–60.
23. S.M.C. Van Bohemen and J. Sietsma: *Mater. Sci. Technol.*, 2009, vol. 25, pp. 1009–12.
24. S.M.C. Van Bohemen and D.N. Hanlon: *Int. J. Mater. Res.*, 2012, vols. 103–8, pp. 987–91.
25. S.M.C. Van Bohemen: *Scripta Mater.*, 2014, vol. 75, pp. 22–25.
26. H. Matsuda and H.K.D.H. Bhadeshia: *Proc. R. Soc. Lond. A*, 2004, vol. 460, pp. 1707–22.
27. S.B. Singh and H.K.D.H. Bhadeshia: *Mater. Sci. Eng., A*, 1998, vol. 245, pp. 72–79.
28. S.V. Parker: PhD Thesis, University of Cambridge, UK, 1997.
29. L.C. Chang and H.K.D.H. Bhadeshia: *Mater. Sci. Technol.*, 1995, vol. 11, pp. 874–81.